Applied Energy 88 (2011) 5083–5089

Contents lists available at ScienceDirect

Applied Energy

journal homepage: www.elsevier.com/locate/apenergy

Parametrical analysis of the design and performance of a solar heat pipe thermoelectric generator unit

Wei He [a,*], Yuehong Su [b], S.B. Riffat [b], JinXin Hou [a], Jie Ji [a]

[a] Department of Thermal Science and Energy Engineering, University of Science and Technology of China, Hefei 230026, China
[b] Institute of Sustainable Energy Technology, Department of Architecture and Built Environment, University of Nottingham, University Park, Nottingham NG7 2RD, UK

ARTICLE INFO

Article history:
Received 11 January 2011
Received in revised form 7 July 2011
Accepted 9 July 2011
Available online 6 August 2011

Keywords:
Constant solar irradiation
Heat pipe (HP)
Thermoelectric generator (TEG)
Parametrical analysis

ABSTRACT

This paper describes a solar heat pipe thermoelectric generator (SHP-TEG) unit comprising an evacuated double-skin glass tube, a finned heat pipe and a TEG module. The system takes the advantage of heat pipe to convert the absorbed solar irradiation to a high heat flux to meet the TEG operating requirement. An analytical model of the SHP-TEG unit is presented for the condition of constant solar irradiation, which may lead to different performance characteristics and optimal design parameters compared with the condition of constant temperature difference usually dealt with in other studies. The analytical model presents the complex influence of basic parameters such as solar irradiation, cooling water temperature, thermoelement length and cross-section area and number of thermoelements, etc. on the maximum power output and conversion efficiency of the SHP-TEG. Simulation based on the analytical model has been carried out to study the performance and design optimization of the SHP-TEG.

1. Introduction

With the diminishing reserve of fossil fuels and the pressing issues of environmental pollution caused by combustion of fossil fuels, research to find new energy sources and affordable new power generation methods has been become more and more important. Compared to conventional electrical power generator systems, thermoelectric generators (TEG) theoretically offer many advantages such as being simple and highly reliable, having no moving parts, and being environmentally friendly. However, they have relatively low conversion efficiencies, so their applications have been usually limited to the specific situations where reliability is a major consideration such as in aerospace and military applications. More recently, there has been a growing interest to use TEG for electricity generation from waste heat of various sources such as combustion of solid waste, power plants, biomass cooking, and other heat-generating processes when the cost of the thermal input do not need to be considered [1–5], and many researches on system optimization and performance improvement of thermoelectric generators for waste heat recovery have been reported in numerous publications [1–10]. In a study, the cost of electricity produced by TEG from waste warm water is predicted to be £0.08/kW h and even to be £0.04/kW h, which can challenge the cost of electricity produced by conventional methods from oil or coal fuels [8].

On the other hand, solar heat driven TEG is emerging as a competing alternative technology to the dominating solar photovoltaic (PV) systems. Though its low conversion efficiency compared to PV, solar-driven TEG technology still attracts increasing attention as other simple and competitive way to produce electricity from solar energy [11–15]. In fact, the low conversion efficiency may be not a serious barrier for use of the free and friendly solar energy. With the decreasing price of thermoelement materials, the TEG technology is attracting more research interest to develop it for solar energy applications and a number of studies on design and optimization of systems and analysis of their performance have been reported in the recent literature. The performance of the TEG in a hybrid PV-TEG system, where the TEG operates independently as a secondary generator to improve the overall efficiency of the system, has been studied [10,11,14]. The analytical method used in these studies are not much different from that used in the study of TEG for waste heat recovery, and calculation of the TEG was based on the temperature difference between the hot side and cool side of a TEG, which was usually chosen at 60 K, 80 K or 100 K. Typically, the thermal conductivity of a TEG is about 1.5 $W\,m^{-1}\,K^{-1}$ and the depth of commercial TEG is about 4 mm (including the ceramic electric insulation), so the heat flux through a TEG could be higher than 20000 $W\,m^{-2}$ for a temperature difference of 60–100 K. However, the solar irradiation is usually less than 1000 $W\,m^{-2}$, which is obviously too low to match the required heat flux of a TEG to obtain a large temperature difference for a considerable efficiency. Solar heat could be accumulated or solar radiation could be concentrated to match the required heat flux of a TEG. A study has used a liquid such as water circulation system

* Corresponding author. Tel.: +86 5513601641; fax: +86 5513606459.
E-mail address: hwei@ustc.edu.cn (W. He).

0306-2619/$ - see front matter © 2011 Elsevier Ltd. All rights reserved.
doi:10.1016/j.apenergy.2011.07.017

Nomenclature

Symbols

A	area, m^2
a	cross-section area of thermoelement, m^2
D	depth or diameter, m
G	solar irradiation, $W\ m^{-2}$
h	heat transfer coefficient, $W\ m^{-2}$
k	thermal conductivity, $W\ m^{-1}\ K^{-1}$
L	length, m
l	length, m
P	power, W
Q	heat flow, W
R	load resistant, Ω
r	electrical resistivity, Ω m
T	temperature
U	voltage, V
W	width, m
δ	Stefan–Boltzmann constant
ε	emissivity
τ	transmissivity
α	absorptivity or Seebeck coefficient, $V\ K^{-1}$

Subscripts

air	air
c	convective
cop	plate copper fin
cross	the cross-section of plate copper fin
load	external load
loss	heat loss from the evacuated glass tube to the environment
in	internal load
r	radiation
sky	sky
tube	glass tube
tube-in	inner glass tube
tube-out	outer glass tube
tegh	ceramic plate of TEG hot side
tegl	ceramic plate of TEG cold side
teg	TEG
f	water flow
hp	heat pipe

to transfer solar heat to a TEG while other studies have investigated use of a line-focus parabolic trough (PTC), a Compound Parabolic Concentrator (CPC) or a two-stage concentrator to provide high density of solar radiation so as to give a high heat flux across the TEG [11,15,16]. A CPC usually has a concentration ratio of less than 5, which is still too low to match the required heat flux of a TEG, so it needs to be used along with a circulation system. Solar tracking parabolic concentrators can easily give a much larger concentration ratio, but the cost of a tracking system could be a barrier and also a TEG may be not competitive to a concentrating PV. Use of a liquid circulation system to transfer solar heat to a TEG is simple, but a larger temperature change of the liquid is required to carry a certain amount of heat, and electricity consumption of the circulation pump and heat loss of the circulation system are other concerns.

And evacuated glass tube solar collectors have become common practice in housing stock worldwide, especially in China. Hot water requirement in winter season should be met according to Chinese system design principle, so it usually leads to too much hot water over normal consumption in summer season, which leads to energy waste. Direct incorporation of a TEG with a heat pipe type evacuated tube solar collector may offer another option for design of solar TEG systems and solar evacuated tube solar collector systems. The presented design of a solar heat pipe TEG (SHP-TEG) system is shown in Fig. 1. The SHP-TEG system can supply hot water, electric power or electric power and hot water simultaneously according to requirement and weather conditions. This paper presents design and electric power performance analysis of a solar heat pipe thermoelectric generator (SHP-TEG), which may lead to a high performance and low cost solar TEG system.

Compared with the common study TEG which has based the energy balance and heat transfer analysis on any given temperatures of the hot and cold junctions of a TEG, in the study of a SHP-TEG, the solar irradiation is known as the input to give a constant heat flux, then the hot and cold junction temperatures and other parameters such as the electric power and efficiency will be determined. Hence, the thermal model and power model in this study will be described for the constant solar irradiation as one of boundary conditions. The effects of solar irradiation, cooling water temperature, the length and cross-section area of thermoelements, and the number of thermoelements on the performance of a SHP-TEG unit will be analyzed. This work was intended to give some guidelines for design and operation of SHP-TEG systems.

2. Mathematical models

It consists of an evacuated glass tube, a heat pipe with heat transfer fin and a thermoelectric module. The A–A cross-sectional view shows the details of the thermoelectric module and the condenser section of the heat pipe. A copper plate is soldered to the condenser of the heat pipe in order to enhance heat transfer, and the thermoelectric module may be bonded to the copper plate tightly using silicon grease. The B–B cross-sectional view shows the detailed structure of the evacuated double-skin glass tube with the heat pipe being inserted. The evacuated space is between the inner tube and the outer glass tube. Besides enhancing heat transfer, the four copper fins on the heat pipe are used as the solar energy absorption surface and also to support the heat pipe inside the inner glass tube. And the heat pipe converts low heat flux to high heat flux by changing the ratio of evaporator area to condenser area. There are three operation models: (1) electrical power priority model, the water temperature in cooling channel 1 keeps low, the cooling channel 2 is empty and closed; (2) electrical power and hot water model, the water temperature in cooling channel 1 meets requirement, the cooling channel 2 is empty and closed; and (3) hot water model, thermoelectric module does not work, cooling channels 1 and 2 are filled with water and the system operates like a normal evacuated tube-heat pipe-solar collector system.

The performance of system operating under model 3 like a normal evacuated tube-heat pipe-solar collector system has been studied in former literatures [17,18]. This study is intended to analyze the steady state performance of the SHP-TEG operating under model 1 or model 2. The heat transfer process across the SHP-TEG is illustrated in Fig. 2. The following assumptions were made to simplify analysis of the complex heat transfer process in the SHP-TEG:

(1) The fins of the heat pipe have the same temperature as the heat pipe.
(2) All the energy balance equations are for the steady state conditions, so the thermal capacity of any parts of the SHP-TEG system is neglected.

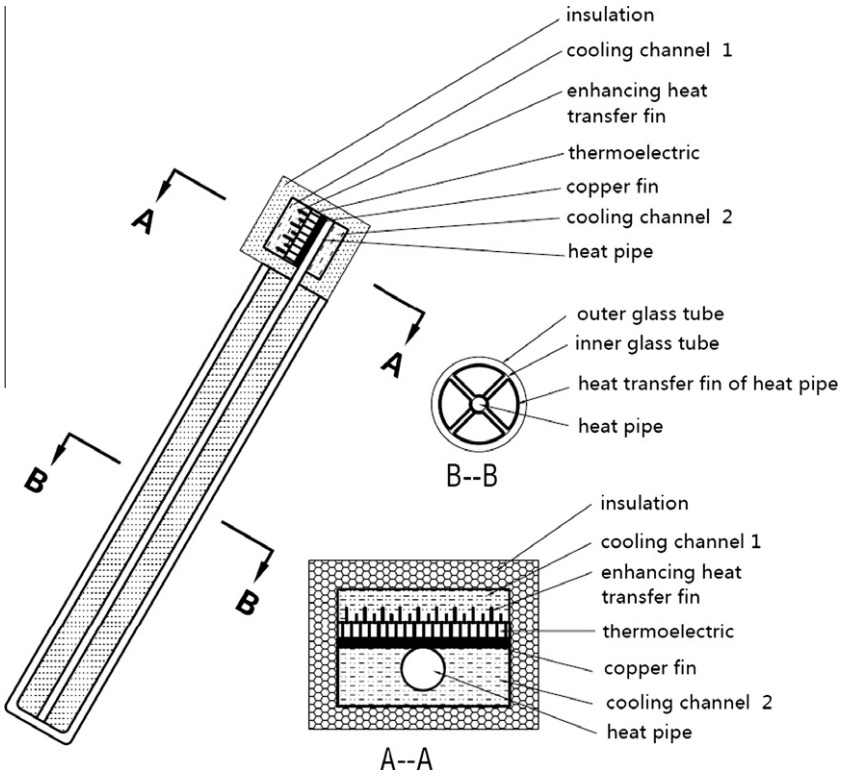

Fig. 1. Schematic of a SHP-TEG.

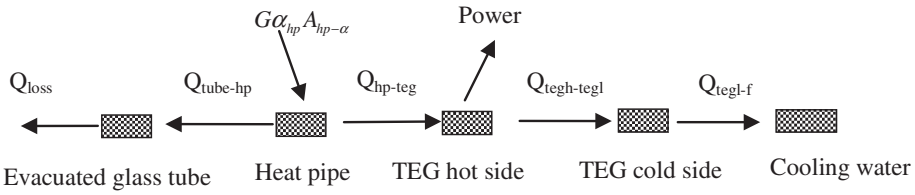

Fig. 2. Schematic of the heat transfer network of the SHP-TEG.

(3) The contact thermal resistance and electric resistance between any two parts of the system are neglected.
(4) The temperature gradient along the heat pipe is neglected.
(5) The section containing the condenser of the heat pipe, the TEG and the water jacket are well insulated without any heat loss to the surroundings.

2.1. Evacuated glass tube

The heat balance of the evacuated double-skin glass tube may be given by:

$$Q_{loss} = h_{c,air}(T_{tube} - T_{air}) + h_{r,sky}(T_{tube} - T_{sky}) = h_{c,tube\text{-}hp}(T_{hp} - T_{tube}) + h_{r,tube\text{-}hp}(T_{hp} - T_{tube}) \quad (1)$$

where Q_{loss} is the heat loss from the evacuated glass tube to the environment, T_{tube} is the surface temperature of the outer tube, T_{hp} is the temperature of the heat pipe, fins and the inner glass tube, T_{air} is the temperature of ambient air, T_{sky} is the sky temperature, $h_{c,a}$ is the convective heat transfer coefficient between the surface of the outer glass tube and the ambient, $h_{r,sky}$ is the radiative heat transfer coefficient between the surface of the outer glass tube and the sky, $h_{c,tube\text{-}hp}$ is the convective heat transfer coefficient between the outer and inner glass tubes, which can be assumed to be zero because of the evacuated space, and $h_{r,tube\text{-}hp}$ is the radiative heat transfer coefficient between the outer and inner glass tube.

The convective heat transfer coefficient between the surface of the outer glass tube and the ambient may be given by $h_{c,air} = 3.8 + 2.7wind$.

The radiative heat transfer coefficient between the surface of the outer glass tube and the sky may be given by $h_{r,sky} = \varepsilon_{tube}\delta\left(T_{sky}^2 + T_{tube}^2\right)\left(T_{sky} + T_{tube}\right)$.

The convective heat transfer coefficient between the outer and inner glass tubes may be given by:

$$h_{r,tube\text{-}hp} = \delta\left(T_{tube}^2 + T_{hp}^2\right)(T_{tube} + T_{hp}) \Big/ \left(1/\varepsilon_{tube\text{-}in} + \frac{A_{tube\text{-}out}}{A_{tube\text{-}in}}(1/\varepsilon_{tube\text{-}out} - 1)\right)$$

where δ is the Stefan–Boltzmann constant and ε_{tube} and ε_{hp} are the emissivity of the outer glass tube and inner glass tube, respectively, $A_{tube\text{-}out}$ is the surface area of the outer glass tube, $A_{tube\text{-}in}$ is the surface area of the inner glass tube. There are:

$$A_{tube\text{-}out} = \pi D_{tube\text{-}out} L_{tube} \quad \text{and} \quad A_{tube\text{-}in} = \pi D_{tube\text{-}in} L_{tube}$$

where $D_{tube\text{-}out}$, $D_{tube\text{-}in}$, L_{tube} are the diameters of the outer and inner tubes and the length of the evacuated glass tube respectively.

2.2. Heat pipe

The temperature gradient along the heat pipe and its fins is neglected. The solar energy absorbed by the heat pipe is converted into heat, most of which is transferred to the condenser part of the heat pipe where the TEG high temperature side is attached to and the rest is transferred to the outer glass tube and then lost to the ambient. The energy balance of the heat pipe may be written as:

$$G\tau_{tube\text{-}out}\alpha_{tube\text{-}in}A_{hp\text{-}\alpha} = h_{r,tube\text{-}hp}A_{hp\text{-}\alpha}(T_{hp} - T_{tube}) + h_{hp\text{-}tegh}A_{coph}(T_{hp} - T_{tegh}) \quad (2)$$

where G is the solar irradiation density, $\tau_{tube\text{-}out}$ is the transitivity of the outer glass tube, $\alpha_{tube\text{-}in}$ is the absorptivity of the inner glass tube, $A_{hp\text{-}\alpha}$ is the heat pipe absorber area, $A_{hp\text{-}\alpha} = D_{tube\text{-}in}L_{tube}$, A_{coph} is the plate copper fin area, $A_{cop} = W_{cop}L_{cop}$, W_{cop}, L_{cop} is the width and length of plate copper fin, T_{tegh} is the temperature of ceramic plate (assumed to be same as the temperature of TEG hot side), and the width and length of ceramic plate are same as that of plate copper fin. $h_{hp\text{-}tegh}$ is the heat transfer coefficient between the heat pipe condenser and the plate ceramic plate of the TEG, as shown in Fig. 1B–B. It is a tube-fin structure and the end of the plate copper fin is well insulated, so the heat transfer coefficient can be written as following:

$$h_{hp\text{-}tegh} = 2\sqrt{h_{cop\text{-}tegh}PL_{cop}k_{cop}A_{cross}}\tanh \times \left(\sqrt{\frac{h_{cop\text{-}tegh}PL_{cop}}{k_{cop}A_{cross}}}\frac{L_{cop}}{2}\right)\Big/(A_{cop}/2) \quad (3)$$

where $h_{cop\text{-}tegh}$ is the heat transfer coefficient between the plate copper fin and the ceramic plate and it is just the average thermal conductivity as expressed as following:

$$h_{cop\text{-}tegh} = 1/(2D_{cop}/k_{cop} + 2D_{tegh}/k_{tegh}) \quad (4)$$

where D_{cop} and k_{cop} is the depth and conductivity of the copper fin respectively, D_{tegh} and k_{tegh} is the depth and conductivity of the ceramic plate respectively, and A_{cross} is the cross-section area of plate copper fin, $A_{cross} = W_{cop}D_{cop}$, $PL_{cop} = 2(W_{cop} + D_{cop})$ is the perimeter of the cross-section of the plate copper fin and it may be simplified to be $PL_{cop} = 2W_{cop}$ neglecting D_{cop}, then Eq. (3) can be rewritten as:

$$h_{hp\text{-}tegh} = 2\sqrt{2h_{cop\text{-}tegh}k_{cop}D_{cop}}\tanh \times \left(\sqrt{h_{cop\text{-}tegh}/(2k_{cop}D_{cop})}\frac{L_{cop}}{2}\right)\Big/(L_{cop}/2) \quad (5)$$

2.3. The hot side of TEG

Heat balance of the hot side of the TEG may be given by:

$$Q_{hp\text{-}teg} = h_{hp\text{-}tegh}A_{coph}(T_{hp} - T_{tegh}) = 2n_{teg}\alpha_{teg}T_{tegh}I + 2n_{teg}\frac{a_{teg}k_{teg}}{l_{teg}}(T_{tegh} - T_{tegl}) - \frac{1}{2}I^2 2n_{teg}\frac{r_{teg}l_{teg}}{a_{teg}} \quad (6)$$

where n_{teg} is the number of thermoelements, α_{teg} is the Seebeck coefficient of thermoelectric materials (p-type and n-type assumed to be same), I is the current, a_{teg} and l_{teg} are the cross-section area and length of thermoelement respectively, r_{teg} and k_{teg} are the electrical resistivity and thermal conductivity of thermoelectric materials, and T_{tegl} is the temperature of the TEG cold side).

2.4. The cold side of TEG

Heat balance of the cold side of TEG may be given by:

$$Q_{teg\text{-}f} = h_{tegl\text{-}f}A_{tegl}(T_{tegl} - T_f) = 2n_{teg}\alpha_{teg}T_{tegl}I + 2n_{teg}\frac{a_{teg}k_{teg}}{l_{teg}}(T_{tegh} - T_{tegl}) + \frac{1}{2}I^2 2n_{teg}\frac{r_{teg}l_{teg}}{a_{teg}} \quad (7)$$

where $h_{tegl\text{-}f}$ is the effective heat transfer coefficient between the ceramic plate and the cooling water and it may be set to be an equivalent constant value, for example 2000 W m^{-2} K^{-1} due to water cooling and heat transfer enhancement of fins, and T_f is the temperature of cooling water.

2.5. Electrical voltage and power

The electrical open circuit voltage of the TEG is given by:

$$U = 2n_{teg}\alpha_{teg}(T_{tegh} - T_{tegl}) \quad (8)$$

The electrical power output is:

$$P = U^2R_{load}/(R_{load} + 2n_{teg}r_{teg}l_{teg}/a_{teg})^2 \quad (9)$$

R_{load} is the load resistance. The electrical power efficiency of the SHP-TEG may be defined as the ratio of the electrical power output to the received solar radiation, that is:

$$\eta = P/(GA_{tube\text{-}out}) \quad (10)$$

3. Simulation

The mathematical model described above was written into a FORTRAN programme to simulate the performance of the SHP-TEG system for different design and operating conditions. The geometrical and physical parameters of the TEG, the heat pipe and the evacuated double-skin glass tube were chosen referring to the general specifications of commercially available components. The parameters used in simulation are listed in Tables 1–3 referring to commercial production and those physical parameters were assumed to be constant in the chosen range of temperatures. The TEG was comprised of a number of Bi2Te3 thermoelements with different cross-section areas. The basic conditions of simulation were set as: the solar irradiation is 1000 W m^{-2}, the cross-section area and the number of thermoelements are 1.4 × 1.4 mm and 127 respectively, the ambient temperature is 25 °C, the wind velocity is 3 m s^{-1}, and the TEG cooling fluid is water.

For the condition of a constant ΔT, the previous studies in the literature have reported that the maximum electrical power of TEG can be achieved when the load resistance equals the internal

Table 1
Geometrical and physical of the TE model.

α_{teg} (V K^{-1})	k_{teg} (W m^{-1} K^{-1})	r_{teg} (Ω m)	k_{tegh} (W m^{-1} K^{-1})	D_{tegh} (m)	D_{tegl} (m)
2.0×10^{-4}	1.5	9.5×10^{-6}	25	0.001	0.001

Table 2
Geometrical and physical parameters of the heat pipe.

L_{hp} (m)	W_{coph} (m)	L_{coph} (m)	D_{coph} (m)	k_{cop} (W m^{-1} K^{-1})
1.8	0.04	0.04	0.002	398

Table 3
Geometrical and physical parameters of the evacuated glass tube.

L_{tube} (m)	$D_{tube\text{-}out}$ (m)	$D_{tube\text{-}in}$ (m)	$\varepsilon_{tube\text{-}out}$	$\tau_{tube\text{-}out}$	$\varepsilon_{tube\text{-}in}$	$\alpha_{tube\text{-}in}$
1.8	0.057	0.047	0.88	0.95	0.06	0.95

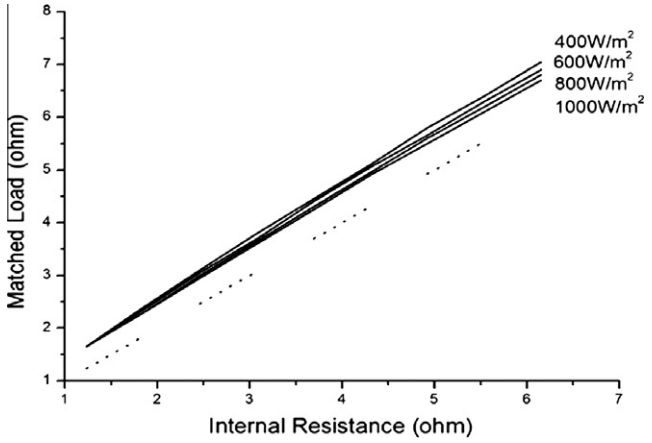

Fig. 3. External load matches internal resistance to get the maximum power output for various solar irradiation values (n_{teg} = 127, T_f = 298 K).

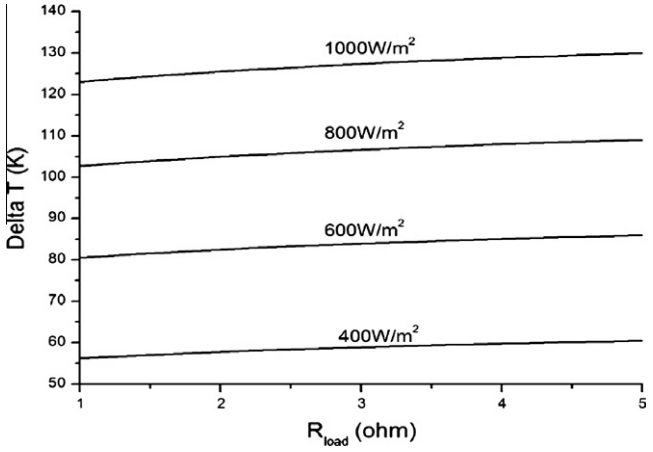

Fig. 4. ΔT vary with load resistance for various solar irradiation values (l_{teg} = 2.5 mm, n_{teg} = 127, T_f = 298 K).

electrical resistance. But for the condition of constant solar irradiation dealt with in the current study, the load resistance R_{load} is not the same as the internal electrical resistance r_{in} when the maximum electrical power is achieved, but a little larger than the internal electrical resistance, as shown in Fig. 3. This could be demonstrated through the following deduction.

Substituting Eq. (8) into Eq. (9) gives a new expression of the power output of a TEG:

$$P = \frac{U^2}{(R_{load}+R_{in})^2}R_{load} = \frac{(2n_{teg}\alpha_{teg})^2\Delta T^2}{(R_{load}+R_{in})^2}R_{load} \tag{11}$$

where the internal electrical resistance is:

$$R_{in} = 2n_{teg}r_{teg}l_{teg}/a_{teg} \tag{12}$$

Differentiating Eq. (11) gives:

$$\frac{dP}{dR_{load}} = \frac{(2n_{teg}\alpha_{teg})^2 R_{load}}{(R_{load}+R_{in})^2}\frac{d(\Delta T^2)}{dR_{load}} + \frac{(2n_{teg}\alpha_{teg})^2\Delta T^2}{(R_{load}+R_{in})^2} - 2\frac{(2n_{teg}\alpha_{teg})^2\Delta T^2 R_{load}}{(R_{load}+R_{in})^3} \tag{13}$$

which should be equal to zero in order to achieve the maximum electrical power output.

For a constant ΔT, if

$$\frac{dP}{dR_{load}} = (2n_{teg}\alpha_{teg})^2\Delta T^2\frac{R_{in}-R_{load}}{(R_{load}+R_{in})^3} = 0 \tag{14}$$

then,

$$R_{load} = R_{in} \tag{15}$$

For the condition of constant solar irradiation G, ΔT varies with R_{load} and the slope is positive, e.g. $\frac{d\Delta T}{dR_{load}} > 0$, as shown in Fig. 4, so if

$$\frac{dP}{dR_{load}} = (2n_{teg}\alpha_{teg})^2\frac{\Delta T^2 R_{in} - \Delta T^2 R_{load} + 2R_{load}(R_{load}+R_{in})\Delta T\frac{d\Delta T}{dR_{load}}}{(R_{load}+R_{in})^3} = 0 \tag{16}$$

Then,

$$\frac{2d\Delta T}{\Delta T dR_{load}}R_{load}^2 + \left(\frac{2R_{in}d\Delta T}{\Delta T dR_{load}} - 1\right)R_{load} + R_{in} = 0 \tag{17}$$

which is complex to get R_{load} expression with R_{in} as variable. In order to get a simple expression of R_{load}, R_{load}^2 was assumed to be $R_{in}R_{load}$. As there is not big difference between R_{in} and R_{load}, this assumption would not cause significant error, so Eq. (17) can be written as:

$$\frac{2}{\Delta T}\frac{d\Delta T}{dR_{load}}R_{in}R_{load} + \left(\frac{2R_{in}}{\Delta T}\frac{d\Delta T}{dR_{load}} - 1\right)R_{load} + R_{in} = 0 \tag{18}$$

$$\text{Thus, } R_{load} = \frac{R_{in}}{1 - \frac{4R_{in}}{\Delta T}\frac{d\Delta T}{dR_{load}}} > R_{in} \tag{19}$$

Eq. (19) shows a clear relationship among R_{in}, R_{load}, ΔT and $\frac{d\Delta T}{dR_{load}}$. As shown in Fig. 4, the $\frac{d\Delta T}{dR_{load}}$ does not change much with variation of the solar irradiation. According to Eq. (19), when a lower solar irradiation leads to a lower ΔT, a larger matched load resistance will be needed, as seen in Fig. 3.

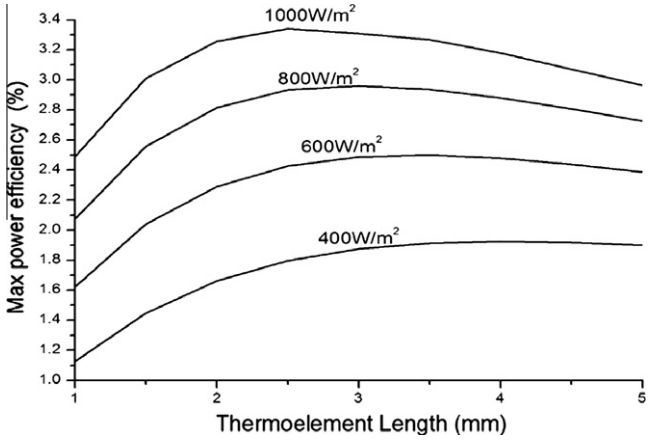

Fig. 5. Max power efficiency changes with TEG length for various solar irradiation values (ambient temperature = 25 °C and cooling water temperature = 25 °C).

Fig. 5 shows variation of the SHP-TEG power conversion efficiency with the change of the solar irradiation and thermoelement length. It can be seen in Fig. 5 that the maximum power conversion efficiency increases with increasing solar irradiation density. For the condition of constant temperature difference between the hot and cold sides of a TEG, the conversion efficiency usually increases with increasing the thermoelement length and the maximum power output will be reduced. But for the condition of constant solar irradiation discussed here the maximum conversion power efficiency has a peak point when varying the thermoelement length and so does the maximum power output according

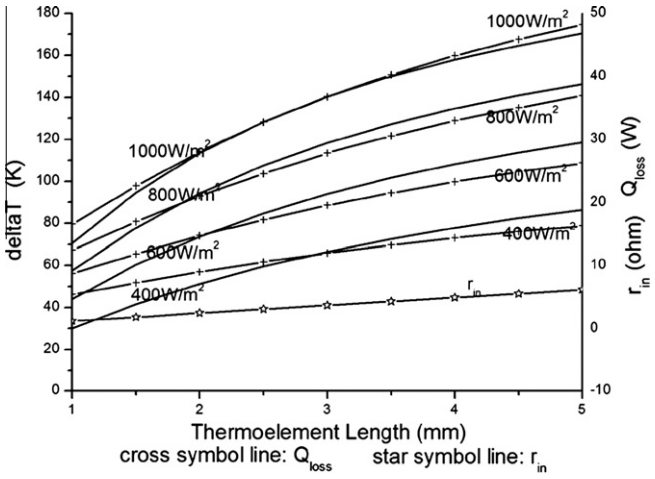

Fig. 6. ΔT and Q_{loss} vary with the thermoelement length for various solar irradiation values and r_{in} vary with the thermoelement length.

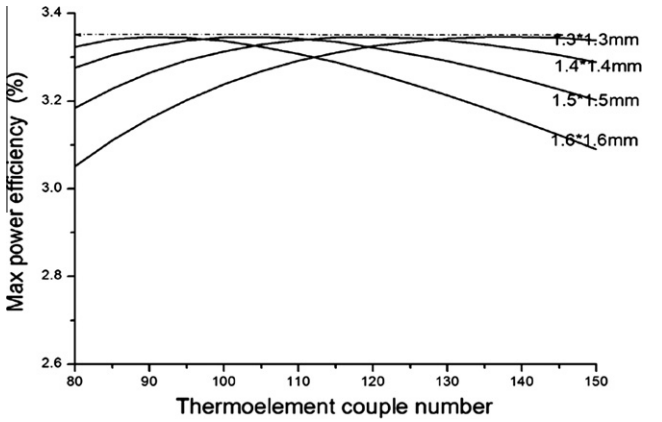

Fig. 7. Maximum power efficiency varies with the number of thermoelements for various cross-section areas of thermoelement ($G = 1000\ \mathrm{W\ m^{-2}}$, $l_{teg} = 2.5$ mm, $T_f = 298$ K).

to Eq. (10). For a given solar irradiation which causes a constant heat flux, a longer thermoelement length means a larger thermal resistance and a larger ΔT, and thus leads a larger operation voltage and higher conversion efficiency. However, when ΔT is larger, the temperature of hot junction also becomes higher, so the operation temperature of heat pipe is higher and heat loss Q_{loss} from the heat pipe to the ambient becomes larger. When the length of thermoelement reaches a certain value, the effect of heat loss will become larger than the effect of increased ΔT, and then the power efficiency becomes to decrease with the length of thermoelement. This could be further explained referring to Fig. 6 which shows ΔT and Q_{loss} variation with the length of thermoelement for different solar irradiation. For example, under the solar irradiation of $1000\ \mathrm{W\ m^{-2}}$, the slope of the curve of Q_{loss} is lower than that of the temperature difference when the thermoelement length is less than 2.5 mm. The two slopes are almost the same when the thermoelement length is around 2.5 mm and then begin to separate after 2.5 mm. This indicates that the thermoelement length 2.5 mm could be a transition point to the performance characteristics of the SHP-TEG and might be the reason why the peak point of conversion efficiency appears at the thermoelement length of about 2.5 mm. under solar irradiation $1000\ \mathrm{W\ m^{-2}}$. It is also evident from Fig. 5 that the position of the peak point of conversion efficiency will change if the solar irradiation is different. For example, under the solar irradiation of $600\ \mathrm{W\ m^{-2}}$, the peak point appears at the thermoelement length of about 3.5 mm compared with 2.5 mm for $1000\ \mathrm{W\ m^{-2}}$. A smaller solar irradiation will give a lower heat flux across the TEG and thus a smaller ΔT and lower operation voltage. As a larger thermoelement length can lead to a larger operation voltage, the thermoelement length will need to be longer to achieve large enough operation voltage under the lower solar radiation.

The internal electrical resistance and thermal resistance of TEG also depend on the number of thermoelements and their cross-section area, and the electric power output will vary with the internal electric resistance and thermal resistance of TEG as analyzed above. Fig. 7 shows the maximum power efficiency of the SHP-TEG varies with the number of thermoelements for various cross-section areas of thermoelements under the conditions of solar irradiation $1000\ \mathrm{W\ m^{-2}}$ and thermoelement length 25 mm. As seen in Fig. 7 that the optimal number of thermoelements decreases with the cross-section area increasing. However, regardless of how the number of thermoelements and cross-section area change, the maximum power efficiency they can achieve is the same and it is 3.346% for the simulation conditions. The optimal number of thermoelements is 139 for 1.3 mm × 1.3 mm, 120 for 1.4 × 1.4, 105 for 1.5 × 1.5, and 92 for 1.6 × 1.6, Multiplying the optimal number of thermoelements and their cross-section area gives the same total area of thermoelements, i.e., about 235 in this case. This means that to achieve the same maximum electrical power efficiency the same amount of thermoelement materials would be required. This provides an important design information for the cost calculation of the SHP-TEG system as the cost of thermoelement materials is a major part in the total cost of a SHP-TEG system.

Fig. 8 shows the maximum power efficiency, the hot and cold side temperatures of TEG and the temperature of heat pipe vary with the temperature of cooling water for $G = 1000\ \mathrm{W\ m^{-2}}$, $l_{teg} = 2.5$ mm, $n_{teg} = 120$. The maximum power efficiency decreases from 3.346% to 2.611% and the temperature of the cold side of TEG increases about 30 K when the temperature of cooling water increases from to 298 K to 328 K, and meanwhile the hot side temperature of TEG is increased by about 10 K which is not as large as that of the cold side of TEG. The maximum power efficiency decreases about 0.12% for every 5 K increase in the temperature of cooling water, so the balance needs to be considered carefully when the SHP-TEG is designed for combined electricity and heat supply applications. Furthermore, when the temperature of cooling water is 328 K, the temperature of the hot side of TEG reaches 450 K which nearly touches the melting point 456 K of tin/lead solder and risks damaging the TEG.

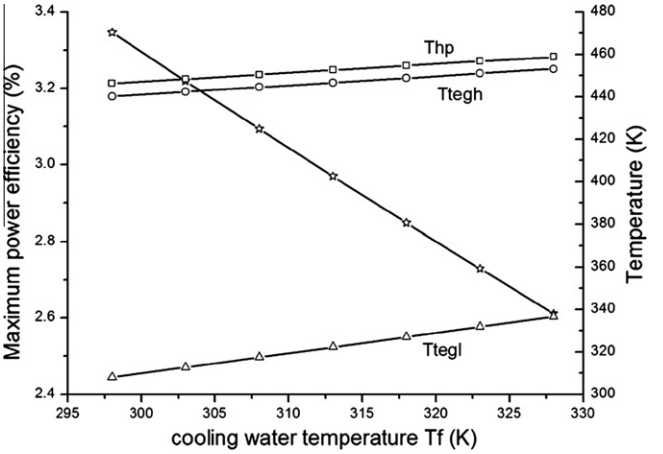

Fig. 8. Maximum power efficiency and temperatures of TEG vary with temperature of cooling water ($G = 1000\ \mathrm{W\ m^{-2}}$, $l_{teg} = 2.5$ mm, $n_{teg} = 120$).

4. Conclusions

An analytical model of the solar heat pipe thermoelectric generator (SHP-TEG) system has been developed for the condition of constant solar irradiation based on operation models 1 and 2, which causes difference performance characteristics and optimal design parameters compared with the condition of a constant temperature difference across a TEG. The analytical model presents the complex influence of basic parameters such as solar irradiation, cooling water temperature, thermoelement length and cross-section area and number of thermoelements, etc. on the maximum power output and conversion efficiency. The analytical model of the SHP-TEG provides a tool for design optimization and performance prediction for the SHP-TEG system. Based on the analytical model, simulation has been carried out to study the performance and design of the SHP-TEG. The simulation shows that there exists a peak point of the maximum power conversion efficiency when the thermoelement length changes and the efficiency of 3.346% can be achieved for 1000 W m^{-2} solar irradiation. To get the maximum power efficiency in the condition of constant solar irradiation, the matched external load resistance is a little larger than the TEG internal electrical resistance. This is difference from the condition of constant temperature difference across a TEG, where the matched external load resistance should be equal to the internal electrical resistance of a TEG.

It is worth mentioning that the factors associated with manufacturing and fabrication processes such as contact thermal resistance, contact electric resistance and temperature dependence of material properties, degrade of material properties, etc. have been neglected in this study, but they are also important to the SHP-TEG system and could be considered in the further performance study of the SHP-TEG.

Furthermore, the transient state performance, long term performance considering degrade of material properties and annual performance analysis of the SHP-TEG system with switching operation model will be performed in next step. As there is a big market of evacuated glass tube solar collector in China, and it is easy to manufacture the SHP-TEG system technically based on a solar evacuated tube solar collector system, with the decreasing price of thermoelement materials, SHP-TEG system will be economical in the near future.

Acknowledgment

The work described in this paper has been supported by the Fundamental Research Funds for the Central Universities (Project No. 2090130002) and the National Nature Science Fund of China (Project No. 51078342).

References

[1] Crane Douglas T, Jackson Gregory S. Optimization of cross flow heat exchangers for thermoelectric waste heat recovery. Energy Convers Manage 2004;45:1565–82.
[2] Champier D, Bedecarrats JP, Rivaletto M, Strub F. Thermoelectric power generation from biomass cook stoves. Energy 2010;35:935–42.
[3] Niu Xing, Yu Jianlin, Wang Shuzhong. Experimental study on low-temperature waste heat thermoelectric generator. J Power Sources 2009;188:621–6.
[4] Gou Xiaolong, Xiao Heng, Yang Suwen. Modeling, experimental study and optimization on low-temperature waste heat thermoelectric generator system. Appl Energy 2010;87:3131–6.
[5] Hsu Cheng-Ting, Huang Gia-Yeh, Chu Hsu-Shen, Yu Ben, Yao Da-Jeng. Experiments and simulations on low-temperature waste heat harvesting system by thermoelectric power generators. Appl Energy 2011;88:1291–7.
[6] Stevens James W. Optimal design of small ΔT thermoelectric generation systems. Energy Convers Manage 2001;42:709–20.
[7] Chen Lingen, Gong Jianzheng, Sun Fengrui, Wu Chih. Effect of heat transfer on the performance of thermoelectric generators. Int J Therm Sci 2002;41:95–9.
[8] Rowe DM, Min Gao. Evaluation of thermoelectric modules for power generation. J Power Sources 1998;73:193–8.
[9] Yu Jianlin, Zhao Hua. A numerical model for thermoelectric generator with the parallel-plate heat exchanger. J Power Sources 2007;172:428–34.
[10] Chen Lingen, Li Jun, Sun Fengrui, Wu Chih. Performance optimization of a two-stage semiconductor thermoelectric-generator. Appl Energy 2005;82:300–12.
[11] Omer Siddig A, Infield David G. Design and thermal analysis of a two stage solar concentrator for combined heat and thermoelectric power generation. Energy Convers Manage 2000;41:737–56.
[12] Rockendorf Gunter, Sillmann Roland, Podlowski Lars, Litzenburger Bernd. PV-hybrid and thermoelectric collectors. Sol Energy 1999;67(4–6):227–37.
[13] Xi Hongxia, Luo Lingai, Fraisse Gilles. Development and applications of solar-based thermoelectric technologies. Renew Sust Energy Rev 2007;11:923–36.
[14] Omer SA, Infield DG. Design optimization of thermoelectric devices for solar power generation. Sol Energy Mater Sol Cells 1998;53:67–82.
[15] Vorobiev Yu, Gonzalez-Hernandez J, Vorobiev P, Bulat L. Thermal-photovoltaic solar hybrid system for efficient solar energy conversion. Sol Energy 2006;80:170–6.
[16] Chow TT. A review on photovoltaic/thermal hybrid solar technology. Appl Energy 2010;87:365–79.
[17] Azad E. Theoretical and experimental investigation of heat pipe solar collector. Exp Therm Fluid Sci 2008;32:1666–72.
[18] Redpath David AG, Eames Philip C, Lo Steve NG, Griffiths Phillip W. Experimental investigation of natural convection heat exchange within a physical model of the manifold chamber of a thermosyphon heat-pipe evacuated tube solar water heater. Sol Energy 2009;83:988–97.